Available online at www.sciencedirect.com
ScienceDirect
International Journal of Heat and Mass Transfer 51 (2008) 1488–1493
International Journal of HEAT and MASS TRANSFER
www.elsevier.com/locate/ijhmt

Technical Note

Numerical investigation of a PCM-based heat sink with internal fins: Constant heat flux

V. Shatikian, G. Ziskind *, R. Letan

Heat Transfer Laboratory, Department of Mechanical Engineering, Pearlstone Center for Aeronautical Studies, Ben-Gurion University of the Negev, P.O. Box 653, Beer-Sheva 84105, Israel

Received 12 January 2007; received in revised form 26 June 2007
Available online 28 January 2008

Abstract

Melting of a phase change material (PCM) is studied in a heat sink with vertical internal fins and a horizontal base to which a constant heat flux is applied. The phase change material is stored between the fins. A detailed parametric investigation explores various fin height and thickness, PCM layer thickness, and applied heat flux. Transient numerical simulations are performed using the Fluent 6 software. The results show how the transient phase change process depends on the heat flux from the base, heat capacity of the PCM, and fin dimensions. Dimensional analysis of the results is performed, and the generalized results are presented in terms of the melt fractions and Nusselt numbers vs. the Fourier, Stefan and Rayleigh numbers.

1. Introduction

Heat-storage capacity of phase change materials (PCMs) is large due to the fact that it is based on the latent heat of melting. However, the low thermal conductivity of many prospective PCMs, especially the organic ones, makes it difficult to utilize this capacity effectively. In order to enhance the rate of heat transfer into PCMs, various techniques have been suggested, like fins, metal and graphite-compound matrices, dispersed high-conductivity particles inside the PCM, and micro-encapsulation.

Lately, the details of heat transfer and phase change in the presence of cooling fins have become the focus of attention [1–4]. Krishnan et al. [4] present an extensive list of references on PCM-based heat sinks reported in the literature. Various approaches were attempted to overcome difficulties that result from complexity and conjunction of the involved physical phenomena, commonly by neglecting one or more essential features of the process, like volumetric expansion due to the phase change, convection in the liquid phase, and motion of the solid in the melt due to density differences, e.g. [5].

A recent study by the authors [6] has overcome these limitations, and solved complete conservation equations simultaneously for the fins, solid and liquid PCM, and air, while allowing for PCM expansion, convection in the melted PCM and air, and solid phase motion in the liquid. There, vertical fins were attached to a constant-temperature horizontal base. Following [6], in the present study melting is explored in essentially the same physical model, illustrated in Fig. 1. However, now a constant heat flux is applied to the horizontal base, to which vertical aluminum fins are attached. The phase change material is stored between the fins. Its properties, including the melting temperature of 23–25 °C, latent and sensible specific heat, thermal conductivity and density in solid and liquid states, are based on a commercially available paraffin wax. Full details of the properties and conditions used for the PCM, aluminum, and air can be found in [6].

A detailed parametric investigation is performed for melting in similar systems with varying fin length, l_f, fin thickness l_t, and PCM layer thickness between the fins, l_b. The ratio l_b/l_t is held constant. The thickness of the base

* Corresponding author. Tel.: +972 8 6477089; fax: +972 8 6472813.
E-mail address: gziskind@bgu.ac.il (G. Ziskind).

0017-9310/$ - see front matter © 2007 Elsevier Ltd. All rights reserved.
doi:10.1016/j.ijheatmasstransfer.2007.11.036

Nomenclature

a, b, c	constants, Eq. (5)
c_p	specific heat of PCM at constant pressure (J/kg °C)
Fo	Fourier number $((k/\rho c_p)t/(l_b/2)^2)$
k	thermal conductivity of PCM (W/m °C)
l	length (m)
L	latent heat of PCM (J/kg)
Nu	Nusselt number $((q''_w/\Delta T)((l_b/2)/k))$
q''	heat flux (W/m^2)
Ra^*	modified Rayleigh number $(g\beta\rho^2 c_p q''_w l^4/k^2\mu))$
Ste^*	modified Stefan number $(q''_w c_p(l_b/2)/(kL))$
t	time (s)
T	temperature (°C or K)

Greek symbols

β	volumetric expansion coefficient of PCM (1/K)
Δ	difference
μ	dynamic viscosity of PCM (kg/m s)
ρ	density of PCM (kg/m^3)

Subscripts

b	PCM width
f	fin length
w	wall
t	fin width

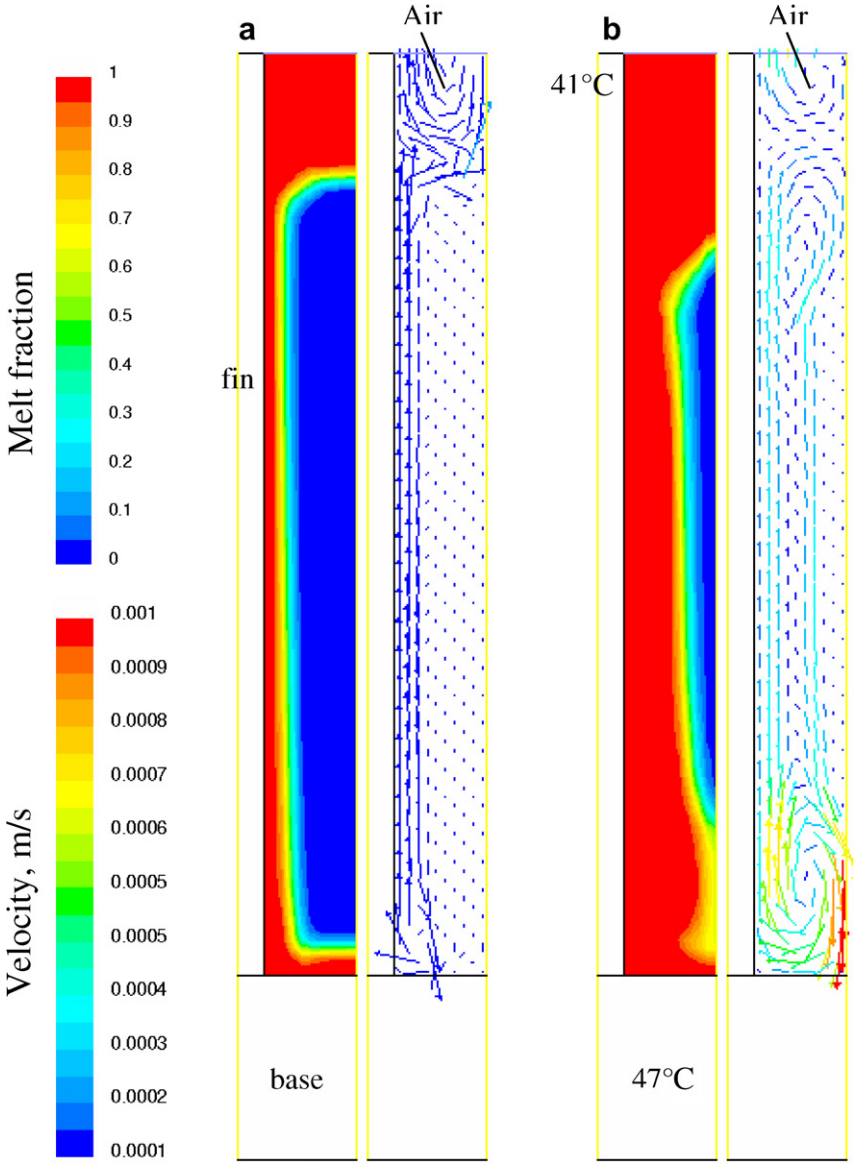

Fig. 1. Examples of simulated phase distributions and velocity fields: (a) melt fraction of 0.2 for case 2, $l_f = 10$ mm and $q''_w = 50$ kW/m^2; (b) melt fraction of 0.65 for case 2, $l_f = 10$ mm and $q''_w = 50$ kW/m^2.

Table 1
Geometry parameters

Case	l_f (mm)	l_t (mm)	l_b (mm)
1	10	1.2	4
2	10, 15, 20	0.6	2
3	10	0.3	1

is 2 mm in all cases considered. The geometrical properties are summarized in Table 1.

For each of the cases in Table 1, calculations are performed for three values of the constant heat flux at the base, namely 25, 50, and 75 kW/m^2. In the simulations, these fluxes are set at $t = 0$ and kept constant through the entire process. The initial temperature of the whole system is 20 °C, i.e. the PCM is slightly subcooled. Ambient air above the unit is kept at 27 °C.

The numerical approach has been extensively discussed in [6]. A "volume-of-fluid" (VOF) model is used to describe the PCM–air system with a moving internal interface. For the phase change region inside the PCM, the enthalpy-porosity approach was used. As shown by Bertrand et al. [7], enthalpy methods are suitable for phase change problems where a solid–liquid interfacial region is present between the phases.

The computational grid was built of 13 cells in the horizontal direction, and this number was kept constant, while the size of the system itself varied. In the vertical direction, there were 120 cells for $l_f = 10$ mm and 220 cells for $l_f = 20$ mm, including 20 cells for the base in each case. Thus, the maximum grid size was $13 \times 220 = 2860$ cells. It was chosen based on the careful analysis of the grid effects on the solution, performed in [6,8]. A significant effort has been dedicated to an analysis of the time step dependence. In addition to the commonly used time step refinement and comparison of the results for different time steps [8], verification of the results has been performed, for every considered case, based on the comparison of the calculated accumulated heat at any instant with the heat supplied to the system. The basic time step was $\Delta t = 0.01$ s, following the analyses of [6,8] for constant wall temperature cases. In cases 1 and 2 with $l_f = 10$ mm, the time step reduction to 0.002 s was found to be sufficient. However, for case 3 with $l_f = 10$ mm, and for case 2 with $l_f = 15$ mm and $l_f = 20$ mm, it was necessary to reduce the time step further, namely to 0.0005 s, meaning that up to $O(10^5)$ time steps were needed in some cases in order to achieve full melting. Fairly accurate balances have been obtained for all cases considered herein, except for case 3, $l_f = 10$ mm and $q''_w = 25$ kW/m^2, which has been excluded from further consideration. The numerical solution has been obtained using the Fluent 6 software. A Pentium 4 computer (CPU 3.00 GHz, 1.0 Gb of RAM) has been used.

2. Results and analysis

Examples of the simulated phase distributions and flow are shown in Fig. 1a and b, for the initial and advanced stages of melting in case 2, $l_f = 10$ mm and $q''_w = 50$ W/m^2, with the melt fractions of about 0.2 and 0.65, respectively. The observed melting patterns are, in general, quite similar to those discussed in [6]. At early stages the melting fronts are almost parallel to the base and the fins, indicating that the fin is already almost isothermal. The flow inside the molten PCM is weak and does not have a significant impact on the melting process. Thus, the liquid layer presents mainly an additional resistance to the heat transfer from the base and fins to the solid PCM. Fig. 1b shows that later the flow becomes relatively strong, affecting not only the melting rate, but also the shape of the remaining solid phase. Counter-rotating vortices in the lower and upper parts of the domain are characteristic to relatively wide cases, and erode the remaining solid phase from both above and below. In narrow cases, the flow patterns preserve their features, characteristic to the early stages of melting, also at the advanced stages. Thus, it can be concluded that the width of the system has a considerable impact on the features of the melting process. On the other hand, for the given fin and PCM thickness in the range considered in the present study, the height of the system does not have a significant effect on the features of the melting process.

Dimensional analysis applied herein in general follows the approach suggested in [6]. However, the constant heat flux situation requires some special definitions when the relevant dimensionless groups are considered. Two dependent dimensionless parameters can be useful [6]: (1) the melt fraction of the PCM, which reflects the heat accumulated by the PCM through the process of phase change; and (2) the Nusselt number, which reflects the time-dependent relation between the instantaneous heat flux and temperature difference. Accordingly, it is defined as

$$Nu = \frac{q''_w}{\Delta T} \cdot \frac{(l_b/2)}{k} \tag{1}$$

being based on the given heat flux, q''_w, temperature difference between the base and the PCM mean melting temperature, ΔT, half-thickness of the PCM layer, $l_b/2$, and thermal conductivity of the PCM, k. Thus, in the present situation the flux is constant while the temperature difference varies, whereas in [6] the same definition reflected the constant temperature difference and variable (dependent) heat flux.

As for the governing dimensionless groups, we define the Fourier number as $Fo = (k/\rho c_p)t/l^2$, where c_p is the specific sensible heat of the PCM, ρ is its density, and t is time. Consistent with [6], a half-thickness of the PCM layer, $l_b/2$, is chosen as the characteristic length, l. To account for the phase change processes, the Stefan number should be involved in the analysis, too. Usually, it is defined as $Ste = c_p \Delta T/L$, where L is the specific heat of melting. However, in the present case the temperature of the base is a dependent variable not known a priori. For this reason, an alternative definition of the Stefan number should be used. Thus, we follow Zhang and Bejan [9] and Pal and

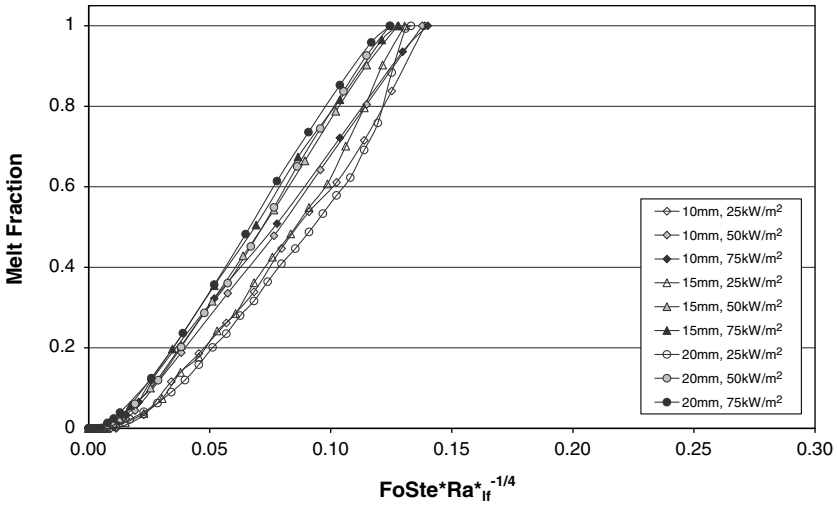

(a) case 2, l_b =2 mm, with various fin heights.

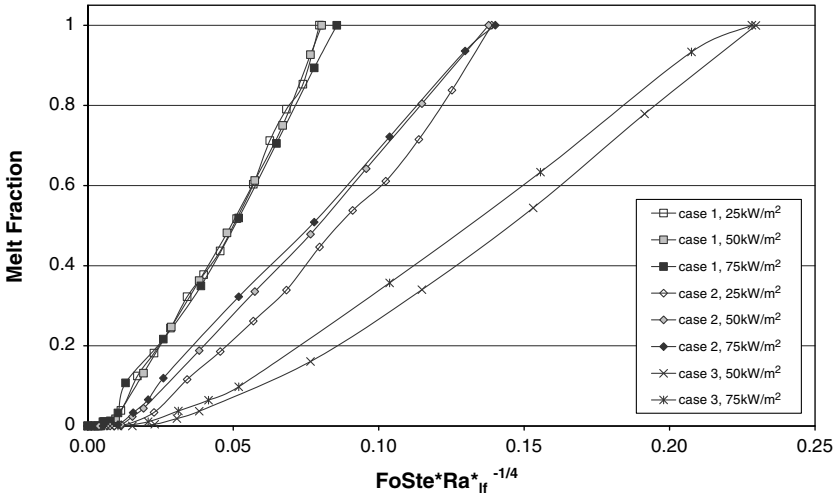

(b) various cases with constant fin height, l_f =10 mm.

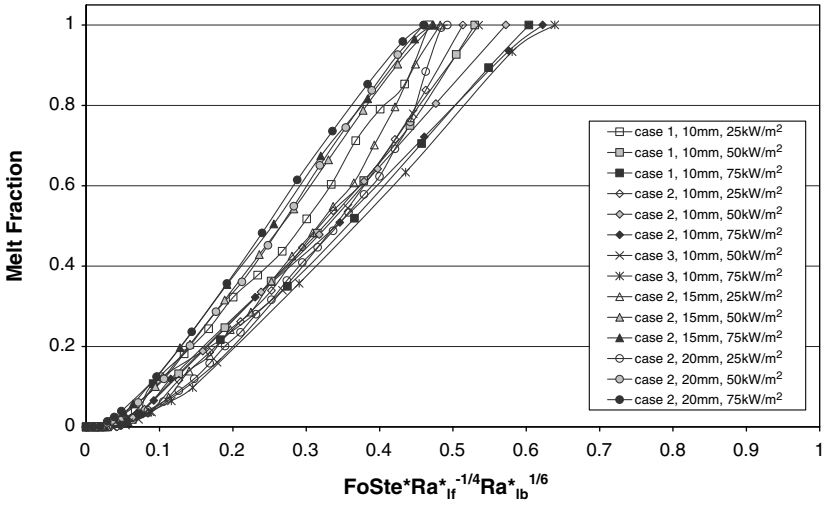

(c) all cases with width-based Rayleigh number.

Fig. 2. Generalized results for the melt fraction at various heat fluxes.

Joshi [10] and define a modified Stefan number, Ste^*, based on the constant heat flux, as

$$Ste^* = \frac{q''_w c_p (l_b/2)}{kL} \tag{2}$$

The product of the Fourier and modified Stefan numbers, $FoSte^*$, takes into account the transient heat conduction and phase change and replaces its commonly used counterpart, $FoSte$, which can be derived from a theoretical analysis of the constant-temperature case. This product cannot account for the effects of heat convection in the melt. In agreement with [6], these effects play an important role when the same geometrical case with various heat inputs is considered, because a higher heat input leads to a more intensive motion in the liquid phase. Following the approach suggested in [6] for the separate geometrical cases, the Rayleigh number is included in the analysis. As in that study, it is based on the fin length, l_f. However, since a constant heat flux is applied to the system, now the modified Rayleigh number, Ra^*, should be defined based on the flux

$$Ra^*_{l_f} = \frac{g\beta\rho^2 c_p q''_w l_f^4}{k^2\mu} \tag{3}$$

where $\beta = 0.001\ K^{-1}$ is the volumetric expansion coefficient, and μ is the dynamic viscosity. The density and dynamic viscosity of the liquid PCM are taken at 25 °C, i.e. correspond to complete melting of the material.

Fig. 2a and b shows the melt fraction in all cases vs. a combination of the Fourier, modified Stefan and modified Rayleigh numbers, namely $FoSte^* Ra^{*-1/4}_{l_f}$. Fig. 2a shows that for various fin heights, all the curves converge for the same base width. This result agrees well with the above-mentioned similarity of the flow patterns for the different heights. We note here that the results of Fig. 2a could be even closer to each other if the Rayleigh number were applied not from the start but rather from the point where the curves begin to diverge due to the emerging convection [6]. On the other hand, Fig. 2b clearly shows that while the melt fraction curves for different heat fluxes almost coincide for each separate case, for various PCM layer widths the results remain clearly separated for the three cases studied. Our previous study [6] indicated that fin efficiency could be considered in search for generalization. However, in the present cases temperature variation along the fins is essentially the same, namely 5–6 °C, as indicated in Fig. 1. This result means that under the conditions considered herein, there is no difference in behavior of the fins 0.3–1.2 mm wide. Thus, it appears that the differences between various geometrical cases cannot be accounted here using the fin parameters.

Motion in the liquid phase is much stronger in the wide cases than in narrow ones. However, the Rayleigh number based on the height, Eq. (3), cannot reflect this phenomenon. Therefore, a parameter is needed that would account for convection dependence on the width of the PCM layers. We assume that one way to account for the width-related convection, e.g. the vortices shown in Fig. 1b, is by defining an additional Rayleigh number, based on the width of the PCM layer, l_b, i.e.

$$Ra^*_{l_b} = \frac{g\beta\rho^2 c_p q''_w (l_b/2)^4}{k^2\mu} \tag{4}$$

Fig. 2c shows the melt fractions of all the cases considered vs. the combination of $FoSte^* Ra^{*-1/4}_{l_f} Ra^{*1/6}_{l_b}$. It appears that the curves for different cases do not converge fully. However, a comparison with Fig. 2b shows clearly that the differences between the cases have become much smaller, indicating that the width-related convective motion indeed plays an important role in the differences between wide and narrow systems. Except for the short initial period of sensible heating, the curves are rather close to a straight line, because the total heat input increases linearly in time.

Finally, Fig. 3 presents the corresponding Nusselt numbers, defined by Eq. (1), for all the cases considered herein. They are shown vs. the same dimensionless combination as

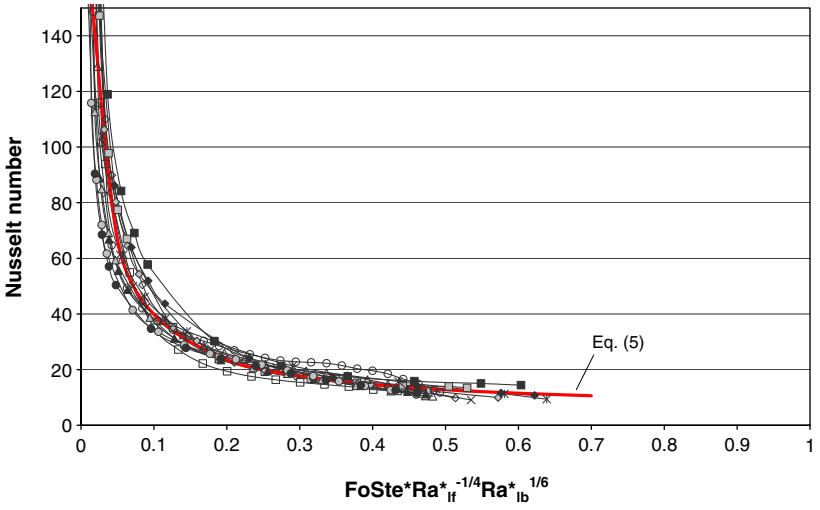

Fig. 3. Generalized results and correlation for the Nusselt number.

in Fig. 2c, $FoSte^{*}Ra_{l_f}^{*-1/4}Ra_{l_b}^{*1/6}$. One can see that a remarkable agreement between the different cases has been achieved. For all cases explored, the Nusselt number is very high at the initial stage of melting, because the thermal resistance is small there. Later, Nu decreases steeply, and after the melt fraction of about 0.2 has been achieved, it continues to decrease asymptotically, approaching a non-zero value that corresponds to heat transfer to a completely melted PCM. Accordingly, the results summarized in Fig. 3 can be expressed by a simple correlation in the form

$$Nu = a + \frac{b}{X + c} \tag{5}$$

where $X = FoSte^{*}Ra_{l_f}^{*-1/4}Ra_{l_b}^{*1/6}$, and a, b, c are constants in our system. Under the present conditions, the best fit is achieved for $a = 5$, $b = 4$, and $c = 0.015$, as also shown in Fig. 3.

3. Conclusions

In the present work, melting of a phase change material (PCM) in a heat sink with a constant heat flux horizontal base and vertical internal plate fins has been studied numerically. It has been shown that within the same geometry, the melt fraction depends on a combination of the Fourier, modified Stefan and modified Rayleigh numbers, where the modified groups are based on the constant heat flux. This result corresponds, in general, to the previous findings for the constant-temperature case of the same configuration. However, it appears that for a constant heat flux at the base, fin efficiency considerations could not be used for generalization. It is therefore suggested to account for the width effect using an additional Rayleigh number, based on the half-width of the PCM layer. The complete results show that a fairly good generalization has been obtained for the melt fraction, while for the corresponding Nusselt numbers the agreement for different cases is very good and a correlation is suggested. The results achieved for constant-temperature and constant heat flux cases show that the suggested dimensional analysis yields consistent results in the both situations. Thus, the approach developed herein can be used in the design of PCM-based cooling systems.

References

[1] H. Inaba, K. Matsuo, A. Horibe, Numerical simulation for fin effect of a rectangular latent heat storage vessel packed with molten salt under heat release process, Heat Mass Transfer 39 (2003) 231–237.
[2] P. Lamberg, K. Siren, Analytical model for melting in a semi-infinite PCM storage with an internal fin, Heat Mass Transfer 39 (2003) 167–176.
[3] P. Lamberg, K. Siren, Approximate analytical model for solidification in a finite PCM storage with internal fins, Appl. Math. Model. 27 (2003) 491–513.
[4] S. Krishnan, S.V. Garimella, S.S. Kang, A novel hybrid heat sink using phase change materials for transient thermal management of electronics, IEEE Trans. Compon. Pack. Technol. 28 (2005) 281–289.
[5] P. Lamberg, R. Lehtiniemi, A.-M. Henell, Numerical and experimental investigation of melting and freezing, processes in phase change material storage, Int. J. Therm. Sci. 43 (2004) 277–287.
[6] V. Shatikian, G. Ziskind, R. Letan, Numerical investigation of a PCM-based heat sink with internal fins, Int. J. Heat Mass Transfer 48 (2005) 3689–3706.
[7] O. Bertrand, B. Binet, H. Combeau, S. Couturier, Y. Delannoy, D. Gobin, M. Lacroix, P. Le Quéré, M. Médale, J. Mencinger, H. Sadat, G. Vieira, Melting driven by natural convection. A comparison exercise: first results, Int. J. Therm. Sci. 38 (1999) 5–26.
[8] E. Assis, L. Katsman, G. Ziskind, R. Letan, Numerical and experimental study of melting in a spherical shell, Int. J. Heat Mass Transfer 50 (2007) 1790–1804.
[9] Z. Zhang, A. Bejan, Melting in an enclosure heated at constant rate, Int. J. Heat Mass Transfer 32 (1989) 1063–1076.
[10] D. Pal, Y.K. Joshi, Melting in a side heated tall enclosure by a uniformly dissipating heat source, Int. J. Heat Mass Transfer 44 (2001) 375–387.